Nanoprobes: Quantitatively Detecting the Femtogram Level of Arsenite Ions in Live Cells

ARTICLE *in* ACS NANO · JUNE 2011

Impact Factor: 12.88 · DOI: 10.1021/nn200994r · Source: PubMed

10 AUTHORS, INCLUDING:

Ru Liu
Chinese Academy of Sciences
28 PUBLICATIONS **459** CITATIONS
SEE PROFILE

Yaling Wang
Chinese Academy of Sciences
24 PUBLICATIONS **228** CITATIONS
SEE PROFILE

Yuliang Zhao
Chinese Academy of Sciences
345 PUBLICATIONS **12,020** CITATIONS
SEE PROFILE

Xueyun Gao
Chinese Academy of Sciences
86 PUBLICATIONS **2,981** CITATIONS
SEE PROFILE

Nanoprobes: Quantitatively Detecting the Femtogram Level of Arsenite Ions in Live Cells

Ru Liu, Zhong Chen, Yaling Wang, Yanyan Cui, Huarui Zhu, Ping Huang, Wei Li, Yuliang Zhao,* Ye Tao, and Xueyun Gao*

CAS Key Lab for Biologic Effects of Nanomaterials and Nanosafety and Beijing Synchrotron Lab Institute of High Energy Physics, Chinese Academy of Science, Beijing 100049 P. R. China

ABSTRACT In this report, nanoprobes which could detect the femtogram level of arsenite ions in subcellular organelle of live cells are disclosed. The nanoprobes are composed of ssDNA and single-wall carbon nanotubes (SWCNTs), and the ssDNA is marked by a dye molecule. In a live cell, trace arsenite ions could interact with nanoprobes and significantly decrease the emission of the nanoprobes. With the help of a confocal microscope and cryo-electron microscopy, the lysosome target of the arsenite ion and nanoprobe is well described in high spatial resolution.

KEYWORDS: nanoprobe · femtogram · live cell · arsenite ion · SWCNTs · ssDNA

In live cells the native metal ions play many important roles, including maintaining enzyme activity, assisting signal transduction, keeping molecular structure stabilization, and capturing small molecules, *etc.*[1−5] To well elucidate the functions of native metal ions in live cells, chemical probes are developed to track their distribution *via* spatial, temporary, and quantity parameters.[6−9] However, traditional chemical probes cannot detect the trace metal ions which are artificially administrated in live cells,[6−9] as they cannot provide high spatial resolution and high sensitivity information of these trace metal ions in the live cell.

Normally trace metal ions are applied in cancer therapy as they play key roles in the control of apoptosis of cancer cells.[10−15] However, their distribution in a live cancer cell has not been well disclosed yet, and the lack of such information hinders researchers in understanding how trace metal ions work in a live cell. For example, arsenite (As) is applied to treat cancers, and several molecular mechanisms have been proposed in past decade, including arsenite inducing cell apoptosis *via* reactive oxygen species, ubiquitin-proteasome pathways, and proteases releasing from lysosome, respectively.[10−16] Note that all these molecular mechanisms are contrary with each other and they all focus on the biomolecular pathway triggered by As; no solid information of arsenite in live cells is supplied to match these molecular mechanisms, therefore it is hard for researchers to describe the correct molecular mechanism of how the arsenic killed the cancer.

In this paper, we design the fluorescent nanoprobe, single-strand DNA wrapped single-wall carbon nanotubes (ssDNA−SWCNTs, the ssDNA is labeled by the dye molecule), to detect the spatial and quantitative distribution of arsenite ions in live cells. Our studies showed the nanoprobes could detect the femtogram (fg) level of arsenite ions in the lysosome of a live cell. The method to prepare and characterize nanoprobes is disclosed in Supporting Information section S1-1, and the HRTEM images in Figure S0 show the clear morphology of ssDNA-SWCNTs.

RESULT AND DISCUSSION

We first disclose the mechanism of how nanoprobes detect the arsenite in Scheme 1. For the nanoprobe, the SWCNT is wrapped by ssDNA, and the ssDNA is labeled by the 5′-hexachloro-fluorescein phosphoramidite (HEX). In a live cell the nanoprobe can emit red when its HEX is excited by light.[17,18] In a live cell, arsenite ions could strongly bind the G/T bases of ssDNA and decrease the $\pi-\pi$ interaction between ssDNA and SWCNTs (see HRTEM and EDS studies in Figure S1-1 of Supporting Information). This makes some ssDNA dissociate from the SWCNTs and further adapt condensed conformation in the live cell (see the SRCD and AFM studies of the nanoprobe working mechanism in Supporting Information section S2). Such condensed conformation of ssDNA will cause the HEX to interact with G/T base-binding arsenite ions, and further induce metal ions quenching the emission of HEX.[19−24] Thus, the nanoprobes can detect arsenite ions *via* an emission decrease method in a live cell.

* Address correspondence to zhaoyuliang@ihep.ac.cn, gaoxy@ihep.ac.cn.

Received for review March 15, 2011 and accepted June 2, 2011.

Published online June 02, 2011
10.1021/nn200994r

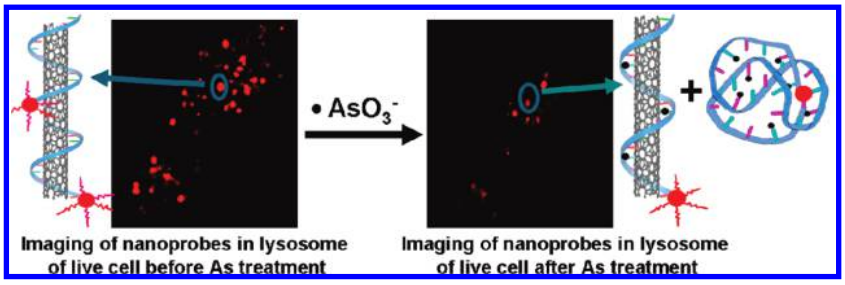

Scheme 1. Illustration of nanoprobes interaction with arsenite ions in a live cell. The arsenite ions bind G/T bases of ssDNA, resulting in some ssDNA to dissociate from the SWCNTs and further condense in the live cell. The emission intensity of the nanoprobe is decreased because the metal ions quench the emission of HEX in condensed ssDNA.[19−24]

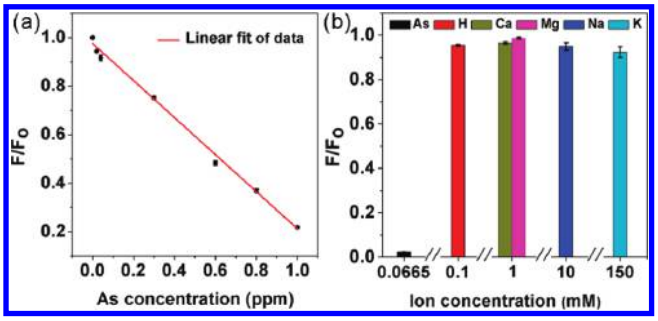

Figure 1. (a) Linear relation between the relative emission intensity of nanoprobes (F/F_0) and the concentration of arsenic. The concentration of As is from 0.02 to 1 ppm, the F/F_0 is from 0 to 1, and the nanoprobe concentration is fixed at 250 nM. (b) The relative emission intensity of nanoprobes when they are incubated with different metal ions, respectively, the K^+ is at 150 mM, Na^+ is at 10 mM, Ca^{2+} and Mg^{2+} are at 1 mM, H^+ is at 0.1 mM, and As is at 0.0665 mM, representing concentrations as found in a live cell.[13,14,25−28] The nanoprobe concentration is fixed at 250 nM in all studies. This result revealed that only arsenite could specifically decrease the emission intensity of the nanoprobes.

First, the numerical relation between concentration of arsenite ions and relative emission intensity of nanoprobes are studied *in vitro* (see methods in Supporting Information section S1-2-1). In Figure 1a, we can see the linear relation between the arsenic concentration and relative emission intensity of nanoprobe *in vitro* (In Figure 1a, the relative emission intensity of nanoprobe is defined as F/F_0, where the F_0 and F are the emission intensity of nanoprobe before and after As-binding, respectively). To verify that the nanoprobe could specifically detect arsenite ions but not native metal ions in live cells, H, Na, K, Ca, Mg ions are incubated with nanoprobes *in vitro*, and the relative emission intensity of the nanoprobes are measured, respectively (see Supporting Information section S1-2-2).[6,25−28] In Figure 1b, we can find that the decrease of F/F_0 induced by native metal ions is negligible as the F/F_0 remains over about 93%, but the decrease of F/F_0 induced by trace arsenite ions is significant, and its value is only about 2%. These data implied native metal ions could not interact with nanoprobes, but arsenite may specifically bind the nanoprobe. Inspired by these data, the binding affinity between the arsenite ion and the nanoprobe is further studied (see Supporting Information SI-3). The binding affinity constant (K_b) is about $1.55 \times 10^5\ M^{-1}$, and this confirms that the arsenite ions could strongly and specifically interact with the nanoprobes.[20] For nanoprobes, the dynamic process of F/F_0 is also a key parameter to be considered when they are applied in arsenite detection. The dynamic process of F/F_0 *in vitro* was studied, and the result is shown in Figure S2 (Supporting Information SI-4). At the beginning stage the F/F_0 of nanoprobes decreased quickly, then became stable as the interaction between the arsenite and nanoprobes reached a balance (see Supporting Information, Figure S2),[29] and finally the F/F_0 of the nanoprobes became stable within 100 s. This result shows that the arsenite ions could quickly bind the nanoprobes and reach a reaction balance, which makes the nanoprobes advantageous in detecting As in live cells.

Although the aforementioned studies ensure that nanoprobes have the potential ability to detect arsenite ions in live cells, their cell toxicity and location in a live cell should be clarified first. The Hela cell was selected in those studies because As has been well applied in the treatment of Hela cells to disclose the mechanism of cancer cell apoptosis.[13−15] The cell viability was assessed by incubating different amounts of the nanoprobe with the Hela cells (see the toxicity studies of the nanoprobes in Supporting Information section S3). In Figure 2a, Hela cells treated with 50 nM nanoprobes have very good morphology and over 95% cells are alive. When the cells are treated with 75 nM nanoprobes, over 90% of the cells remained viabile (Figure 2a). From the cell viability studies we get the optimized concentration (50nM) and time (36 h) of the nanoprobes for the following cell studies. The location of the nanoprobes in the live Hela cells is observed by the confocal microscope, see Figure 2b. It was found that the red emission of the nanoprobes and

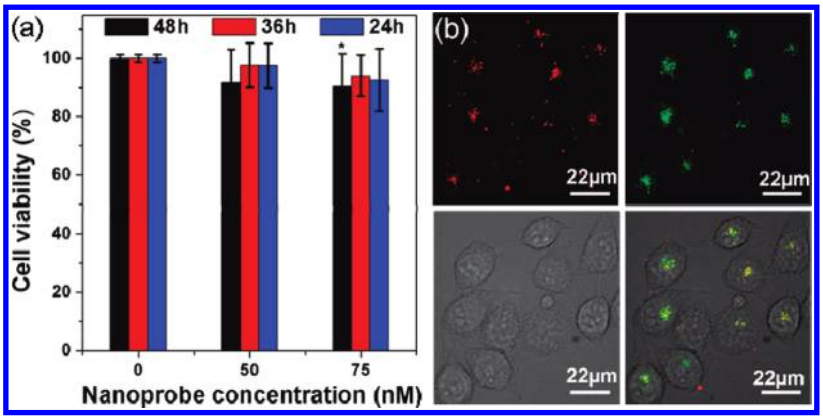

Figure 2. (a) Cell viability when a Hela cell is incubated with nanoprobes for different times; the concentration of nanoprobes is 50 and 75 nM, respectively. The black, red, and blue bar represent 48, 36, and 24 h, respectively. (b) Confocal microscope images of Hela cells incubated with nanoprobes for 36 h. (Top left) red color is from nanoprobes in a live cell, excitation light is 488 nm; (top right) green color is from Lysotracker dyes in lysosome of live cell, excitation light is 514 nm; (bottom left) bright field images of Hela cell; (bottom right) yellow color is from colocalization of nanoprobe and Lysotracker dyes in cell. These images confirmed that the nanoprobes located in the lysosome of live cells. The nanoprobe concentration is 50 nM in culture media.

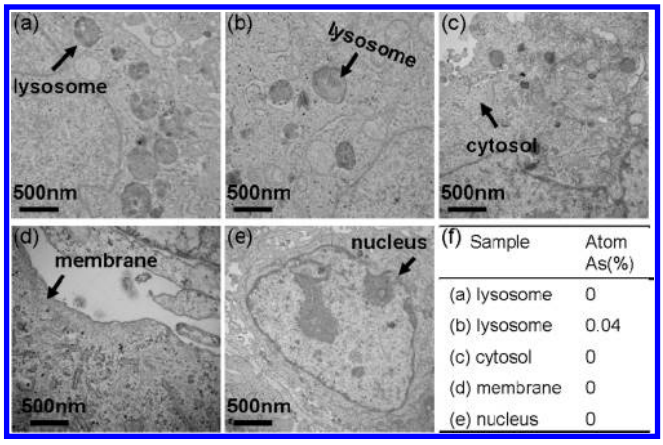

Figure 3. Cryo-TEM images of Hela cells. (a) Control cell without As treatment. (b–e) Different organelles of cells treated by 5 ppm arsenic for 60 min. (f) As signal in different organelles *via* SAEDS studies. In As treated cells, As is found in lysosome only.

the green emission of Lysotracker Green colocalize and overlay very well with each other in a live cell; this means that the nanoprobes are localized in lysosome when the nanoprobes are incubated with the Hela cells. To make sure that the main live cells in the culture media are marked by the nanoprobes, flow cytometry was used to count the cells, and over 76% of the cells were found to be marked by nanoprobes[30] (see S4-1 in Supporting Information). Our further studies also revealed that the nanoprobes are transported into the lysosome of the Hela cells *via* an energy dependent endocytosis process, because either the use of the blocking agent NaN_3 or a decrease in temperature would suppress the nanoprobes moving into the Hela cells (see transport of nanoprobes for Hela cells in S4-2 of Supporting Information). This result also coincides with the previous report.[31]

To verify the nanoprobe could detect the arsenite ions in live cells, the distribution of arsenite ions in the lysosome of Hela cells should be clarified first. Previous toxicity studies of high dosages of As in animal models implied that the As is concentrated in the lysosome.[32,33] To confirm the subcellular location of arsenite ions in live Hela cells, the cells are first incubated with 5 ppm arsenite for 60 min. Note that the time and dosage of arsenite ions in this study match those reported in previous cancer cell studies,[10−16] and these parameters are further optimized in live cell studies (see As toxicity studies in Supporting Information section S3). After the live cells are exposed to 5 ppm arsenite for 60 min, Hela cells are fixed and Cryo-TEM is used to check the lysosome, cell membrane, nucleus, and cytosol including mitochondria and golgi (see Cryo-TEM studies in Supporting Information section S5), and the element components of these organelles are studied by selected area energy dispersive spectra (SAEDS, see the detail SAEDS result in Table S1 of Supporting Information section S5), respectively. In Figure 3, the morphology of these organelles and the arsenic signal in these organelles are disclosed, where the As signal can be only picked up in lysosome of Hela cells treated by As (see Figure 3b,f). It should be noted that there is no As signal in the lysosome of the As free cell (control cell) (see Figure 3a,f). These results confirmed that the As is

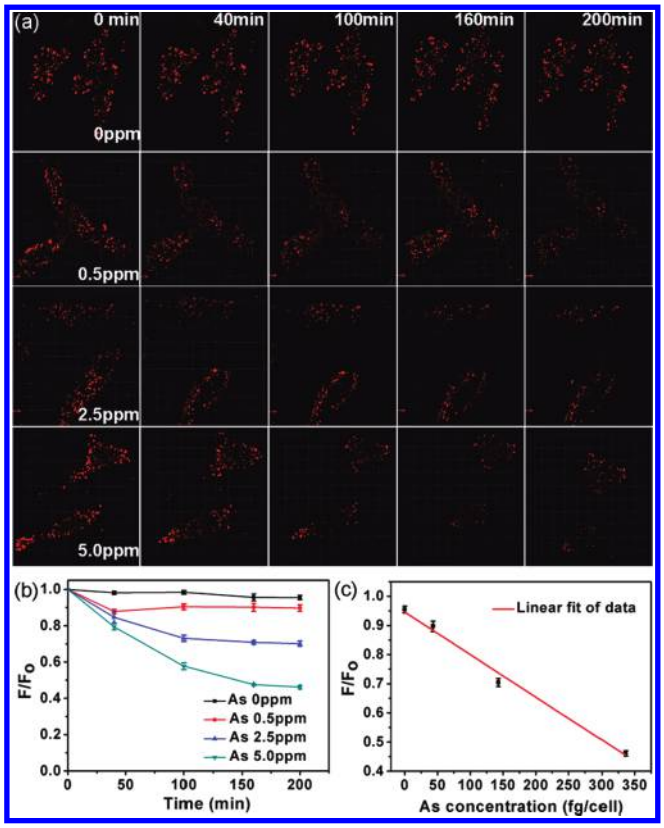

Figure 4. (a) The confocal microscope images of nanoprobes in live cells treated by As. From top to bottom, rows 1, 2, 3, and 4 refer to cells treated by 0 (control), 0.5, 2.5, 5 ppm arsenic, respectively. From left to right, lanes 1, 2, 3, 4, 5 refer to As-cell incubation times of 0, 40, 100, 160, and 200 min, respectively. (b) The relation between time (As-cell incubation time) and relative emission intensity of the nanoprobes in cells. The black, red, blue, and green curves refer to cells treated by 0, 0.5, 2.5, and 5 ppm arsenic, respectively. (c) The linear relation between relative emission intensity of nanoprobes and As concentration in live cells. Triplicate studies were carried out for all experiments.

transported and concentrated in lysosome in live Hela cells when cells are incubated with arsenite.

The aforementioned studies disclosed that both As and nanoprobes colocalize in the lysosome of live Hela cells. This implies that arsenite ions may specifically interact with nanoprobes and induce a decrease in emission in live cells as they did *in vitro* (see Figure 1). In live cells, the As-induced emission decrease of nanoprobes is studied as follows (see method details of confocal microscope studies in Supporting Information, section s6-1). Briefly, the live Hela cells with nanoprobes localized in lysosome are prepared by incubating cells with nanoprobes, then these cells are equally divided into four groups and arsenite ions are introduced into the live cells, where the As concentration is 0 (control), 0.5, 2.5, and 5 ppm, respectively. Once the cell are incubated with As, the emission intensity of the nanoprobes located in the live Hela cells are tracked *in situ* for 200 min. During this tracking process, the emission intensity of the nanoprobes in the live cells is counted at time points 0, 40, 100, 160, and 200 min. The three-dimensional fluorescent images of the nanoprobes located in lysosome are disclosed in Figure 4a, where the As-cell incubation time (from left to right), the As dosage (from top to bottom), and the emission intensity of nanoprobes located in lysosome can be observed. The numerical relation among As-cell incubation time, As dosage, and relative emission intensity of the nanoprobes is shown in Figure 4b. Clearly, for As-free Hela cells (control) the relative emission intensity of the nanoprobes remains stable as there is no As in the live cells (see black curve in Figure 4b, where F/F_0 is about 98% and this value remains stable for the entire confocal observation), this result showed that the emission intensity of the nanoprobes is not disturbed by the native components in live cells. However, Figure 4b showed that the relative emission intensity of the nanoprobes (F/F_0) decreases when As is transported into the Hela cells. The higher dosage of As and longer As-cell incubation time induced more As transport into the lysosome; this result significantly decreases the relative emission intensity of the nanoprobes (see red, blue, and green curves in Figure 4b). For 0.5 ppm As-treated cell the F/F_0 became stable after 50 min, where the F/F_0 is at about 91% in the red curve of Figure 4b. For 2.5 ppm As-treated cells the F/F_0 of the nanoprobes became stable after 160 min, where the F/F_0 is about 72% in the blue curve of Figure 4b. For 5 ppm As-treated cells, the F/F_0 of the nanoprobes became stable after about 180 min, where

the F/F_0 is about 43% in the green curve of Figure 4b. In Figure 4b, the relative emission intensity of nanoprobes becoming stable at different time points implies that arsenite transports into lysosome and interacts with nanoprobes finally reaching a dynamic balance; F/F_0 became stable and the As in higher dosages needed a longer time to reach dynamic balance. Under such dynamic balance, the numerical relation between the relative emission intensity of the nanoprobes and concentration of As in lysosome could be setup as follows. At time point 200 min, the quantity of As in the cells is measured by ion couple plasma mass spectra (ICP–MS), (Supporting Information, section S6-2), and the corresponding relative emission intensity of nanoprobes in lysosome is extracted by confocal microscope (see S6-3). In Figure 4c, the perfect linear relation between relative emission intensity of nanoprobes and amount of As in live cells are setup. According to this relation, we can find that live cells have 40, 140, and 330, fg Arsenic when the cells with 0.5, 2.5, and 5 ppm As, respectively, are incubated for 200 min. This result supported the previous cell studies: cancer cell apoptosis is induced by arsenite; high dosage arsenic will push the cancer cell apoptosis more quickly as more As is concentrated in the cell.[10–16] More importantly, the previous speculation in cell studies, such as the arsenic is concentrated in the lysosome and further triggers the protease pathway to induce cell apoptosis, is strongly supported by our results. In addition, according the relation in Figure 4c, we can calculate the concentration of As in the lysosome of live cells when the relative emission intensity of the nanoprobes in the cells is extracted by confocal microscope.

CONCLUSION

In summary, nanoprobes are demonstrated to detect femtogram level arsenite in the lysosome of live Hela cells, and the spatial distribution of arsenite in live cells, lysosome, is also tracked very well by nanoprobes. For the first time, our studies provide a method to detect artificial metal ions *via* spatial and quantity parameters in live cells. This study also gives clear proof that the target organelle of arsenite is lysosome, and this strong proof can help the molecular researcher determine the right molecular pathway of As-induced cancer cell apoptosis.

Acknowledgment. This work was supported by NSFC (30870677, 31070891), 973 Program (2007CB935604, 2009CB930204, 2011CB933400), and CAS Knowledge Innovation Program).

Supporting Information Available: Experimental details of nanoprobes synthesis, ion selectivity of nanoprobes, ion binding affinity of nanoprobes, dynamic reaction process of nanoprobes, SRCD and AFM studies of nanoprobes working mechanism, cell transport of nanoprobes, toxicity studies of arsenic and nanoprobes in cell, Cyro-TEM studies of arsenic in cell, confocal microscope observation of nanoprobes and count of emission intensity of nanoprobes in cells, ICP–MS studies of As in cells. This material is available free of charge *via* the Internet at http://pubs.acs.org.

REFERENCES AND NOTES

1. Clapham, D. E. Calcium Signaling. *Cell* **2007**, *131*, 1047–1058.
2. Anastassopoulou, J.; Theophanides, T. Magnesium–DNA Interactions and the Possible Relation of Magnesium to Carcinogenesis Irradiation and Free Radicals. *Crit. Rev. Oncol. Hematol.* **2002**, *42*, 79–91.
3. Moenne-Loccoz, P. Spectroscopic Characterization of Heme Iron–Nitrosyl Species and Their Role in NO Reductase Mechanisms in Diiron Proteins. *Nat. Prod. Rep.* **2007**, *24*, 610–620.
4. Kunishita, A.; Kubo, M.; Sugimoto, H.; Ogura, T.; Sato, K.; Takui, T.; Itoh, S. Mononuclear Copper(II)-Superoxo Complexes that Mimic the Structure and Reactivity of the Active Centers of PHM and DβM. *J. Am. Chem. Soc.* **2009**, *131*, 2788–2789.
5. Lucas, H. R.; Meyer, G. J.; Karlin, K. D. Carbon Monoxide and Nitrogen Monoxide Ligand Dynamics in Synthetic Heme and Heme–Copper Complex Systems. *J. Am. Chem. Soc.* **2009**, *131*, 13924–13925.
6. Farruggia, G.; Iotti, S.; Prodi, L.; Montalti, M.; Zaccheroni, N.; Savage, P. B.; Trapani, V.; Sale, P.; Wolf, F. I. 8-Hydroxyquinoline Derivatives as Fluorescent Sensors for Magnesium in Living Cells. *J. Am. Chem. Soc.* **2006**, *128*, 344–350.
7. Domaille, D. W.; Que, E. L.; Chang, C. J. Synthetic Fluorescent Sensors for Studying the Cell Biology of Metals. *Nat. Chem. Biol.* **2008**, *4*, 168–175.
8. Miyawaki, A.; Llopis, J.; Heim, R.; McCaffery, J. M.; Adams, J. A.; Ikura, M.; Tsien, R. Y. Fluorescent Indicators for Ca^{2+} Based on Green Fluorescent Proteins and Calmodulin. *Nature* **1997**, *388*, 882–887.
9. Cheeti, S.; Lee, C. H. The Involvement of Intracellular Calcium in the MCT-Mediated Uptake of Lactic Acid by HeLa Cells. *Mol. Pharm.* **2010**, *7*, 169–176.
10. Zhang, X. W.; Yan, X. J.; Zhou, Z. R.; Yang, F. F.; Wu, Z. Y.; Sun, H. B.; Liang, W. X.; Song, A. X.; Lallemand-Breitenbach, V.; Jeanne, M.; *et al*. Arsenic Trioxide Controls the Fate of the PML-RAR Oncoprotein by Directly Binding PML. *Science* **2010**, *328*, 240–243.
11. Smith, D. M.; Patel, S.; Raffoul, F.; Haller, E.; Mills, G. B.; Nanjundan, M. Arsenic Trioxide Induces a Beclin-1-Independent Autophagic Pathway *via* Modulation of SnoN/SkiL Expression in Ovarian Carcinoma Cells. *Cell Death Differ.* **2010**, *17*, 1867–81.
12. Lallemand-Breitenbach, V.; Jeanne, M.; Benhenda, S.; Nasr, R.; Lei, M.; Peres, L.; Zhou, J.; Zhu, J.; Raught, B.; de Thé, H. Arsenic Degrades PML or PML–RARα through a SUMO-Triggered RNF4/ubiquitin-Mediated Pathway. *Nat. Cell Biol.* **2008**, *10*, 547–555.
13. Kang, Y. H.; Yi, M. J.; Kim, M. J.; Park, M. T.; Bae, S.; Kang, C. M.; Cho, C. K.; Park, I. C.; Park, M. J.; Rhee, C. H.; *et al*. Caspase-Independent Cell Death by Arsenic Trioxide in Human Cervical Cancer Cells: Reactive Oxygen Species-Mediated Poly(ADP-Ribose) Polymerase-1 Activation Signals Apoptosis-Inducing Factor Release from Mitochondria. *Cancer Res.* **2004**, *64*, 8960–8967.
14. Kapahi, P.; Takahashi, T.; Natoli, G.; Adams, S. R.; Chen, Y.; Tsien, R. Y.; Karin, M. Inhibition of NF-kB Activation by Arsenite through Reaction with a Critical Cysteine in the Activation Loop of IκB Kinase. *J. Biol. Chem.* **2000**, *275*, 36062–36066.
15. Chen, Y. C.; Lin-Shiau, S. Y.; Lin, J. K. Involvement of Reactive Oxygen Species and Caspase 3 Activation in Arsenic-Induced Apoptosis. *J. Cell. Physiol.* **1998**, *177*, 324–333.
16. Kitareewan, S.; Roebuck, B. D.; Demidenko, E.; Sloboda, R. D.; Dmitrovsky, E. Lysosomes and Trivalent Arsenic Treatment in Acute Promyelocytic Leukemia. *J. Natl. Cancer Inst.* **2007**, *99*, 41–52.
17. Probert, W. S.; Schrader, M. N.; Khuong, N. Y.; Bystrom, S. L.; Graves, M. H. Real-Time Multiplex PCR Assay for Detection of *Brucella* spp., *B. abortus*, and *B. Melitensis*. *J. Clin. Microbiol.* **2004**, *42*, 1290–1293.
18. Weinert, F. M.; Braun, D. An Optical Conveyor for Molecules. *Nano Lett.* **2009**, *9*, 4264–4267.

19. Gao, X. Y.; Xing, G. M.; Yang, Y. L.; Shi, X. L.; Liu, R.; Chu, W. G.; Jing, L.; Zhao, F.; Ye, C.; Yuan, H.; *et al*. Detection of Trace Hg^{2+} *via* Induced Circular Dichroism of DNA Wrapped around Single-Walled Carbon Nanotubes. *J. Am. Chem. Soc.* **2008**, *130*, 9190–9191.
20. Nafisi, S.; Sobhanmanesh, A.; Alimoghaddam, K.; Ghavamzadeh, A.; Tajmir-Riahi, H. A. Interaction of Arsenic Trioxide As_2O_3 with DNA and RNA. *DNA Cell Biol.* **2005**, *24*, 634–640.
21. Nolan, E. M.; Lippard, S. J. Tools and Tactics for the Optical Detection of Mercuric Ion. *Chem. Rev.* **2008**, *108*, 3443–3480.
22. Rupcich, N.; Chiuman, W.; Nutiu, R.; Mei, S.; Flora, K. K.; Li, Y. F.; Brennan, J. D. Quenching of Fluorophore-Labeled DNA Oligonucleotides by Divalent Metal Ions: Implications for Selection, Design, and Applications of Signaling Aptamers and Signaling Deoxyribozymes. *J. Am. Chem. Soc.* **2006**, *128*, 780–790.
23. Ono, A.; Togashi, H. Highly Selective Oligonucleotide-Based Sensor for Mercury (II) in Aqueous Solutions. *Angew. Chem., Int. Ed.* **2004**, *43*, 4300–4302.
24. Zhao, Y.; Zhong, Z. Q. Modulating the Sensory Response of a Conjugated Polymer by Proteins: An Agglutination Assay for Mercury Ions in Water. *J. Am. Chem. Soc.* **2006**, *128*, 9988–9989.
25. Lubin, M. Intracellular Potassium and Macromolecular Synthesis in Mammalian Cells. *Nature* **1967**, *213*, 451–453.
26. Christensen, K. A.; Myers, J. T.; Swanson, J. A. PH-Dependent Regulation of Lysosomal Calcium in Macrophages. *J. Cell Sci.* **2002**, *115*, 599–607.
27. Negulescu, P. A.; Harootunian, A.; Tsien, R. Y.; Machen, T. E. Fluorescence Measurements of Cytosolic Free Na Concentration, Influx and Efflux in Gastric Cells. *Cell Regul.* **1990**, *1*, 259–268.
28. Geisow, M. J.; D'Arcy Hart, P.; Young, M. R. Temporal Changes of Lysosome and Phagosome pH during Phagolysosome Formation in Macrophages: Studies by Fluorescence Spectroscopy. *J. Cell Biol.* **1981**, *89*, 645–652.
29. Casanova, D.; Bouzigues, C.; Nguyen, T. L.; Ramodiharilafy, R. O.; Bouzhir-Sima, L.; Gacoin, T.; Boilot, J. P.; Tharaux, P. L.; Alexandrou, A. Single Europium-Doped Nanoparticles Measure Temporal Pattern of Reactive Oxygen Species Production inside Cells. *Nat. Nanotechnol.* **2009**, *4*, 581–585.
30. Hai, M.; Bernath, K.; Tawfik, D.; Magdassi, S. Flow Cytometry: A New Method To Investigate the Properties of Water-in-Oil-in-Water Emulsions. *Langmuir* **2004**, *20*, 2081–2085.
31. Kam, N. W. S.; Liu, Z. A.; Dai, H. J. Carbon Nanotubes as Intracellular Transporters for Proteins and DNA: An Investigation of the Uptake Mechanism and Pathway. *Angew. Chem., Int. Ed.* **2006**, *45*, 577–581.
32. Fowler, B. A. General Subcellular Effects of Lead, Mercury, Cadmium, and Arsenic. *Environ. Health Persp.* **1978**, *22*, 37–41.
33. Brown, M. M.; Rhyne, B. C.; Goyer, R. A.; Fowler, B. A. Intracellular Effects of Chronic Arsenic Administration on Renal Proximal Tubule Cells. *J. Toxicol. Environ. Health* **1976**, *1*, 505–514.